

# Continuously Tunable Fractional Hilbert Transformer by Using a Single $\pi$ -Phase Shifted FBG

Hiva Shahoei, *Student Member, IEEE*, and Jianping Yao, *Fellow, IEEE*

**Abstract**—A continuously tunable fractional Hilbert transformer (FHT) using a  $\pi$ -phase shifted fiber Bragg grating ( $\pi$ -PSFBG) is proposed and experimentally demonstrated. An FHT has an output that is a weighted sum of the original input signal and its classical Hilbert-transformed signal. The classical Hilbert transform is implemented using a  $\pi$ -PSFBG. The output from the classical HT and the original input signal are controlled to be orthogonally polarized. The combination of the two signals at a polarizer would generate a weighted sum with the weighting coefficients determined by the angle between the principle axis of the polarizer and the polarization direction of the original input signal. A  $\pi$ -PSFBG is fabricated. The performance of the  $\pi$ -PSFBG as a classical HT is evaluated. The incorporation of the  $\pi$ -PSFBG into the proposed system to implement an FHT is studied. A continuously tunable FHT with a tunable fractional order of  $\rho = 0.7, 0.86, 0.92, 1, 1.06, 1.17, \text{ and } 1.24$  to perform Hilbert transformation of a Gaussian pulse with a temporal width of 80 ps is experimentally demonstrated.

**Index Terms**—Optical signal processing, fractional Hilbert transformer, phase shifted-fiber Bragg grating.

## I. INTRODUCTION

**H**ILBERT transformer (HT) is one of the basic building blocks needed for all-optical signal processing. A HT is also called a quadrature filter which can find numerous applications in radar, communications and modern instrumentation systems [1]. In addition to classical HTs, a fractional Hilbert transformer (FHT) was also demonstrated to generalize the performance of a classical HT with an additional degree of freedom [2]. Thanks to the inherent advantages offered by optics, a HT or FHT can be implemented in the optical domain for high speed and large bandwidth signal processing. In the last few years, different methods have been proposed to demonstrate optical HTs and FHTs. In general, a microwave HT can be realized based on free space optics [2], [3], fiber optics [4]–[11], or photonic integrated circuits [12], [13]. A fiber-optic HT has the advantage of smaller size and light weight, which has been extensively investigated. For example, a HT can be implemented using a multitap photonic transversal filter [4]–[7], or a fiber Bragg grating (FBG) [8]–[10]. In [4], [5],

a microwave delay-line filter with three taps was proposed to implement a classical microwave HT in which the negative taps of the filter were generated by two Mach-Zehnder modulators (MZMs) biased at the complementary quadrature bias points. In [6], an FHT based on a five-tap photonic delay-line filter using a polarization modulator (PolM) was proposed in which the negative taps were generated based on phase inversion by polarization-modulation to intensity-modulation conversion. In [7], a tunable FHT based on a nonuniformly spaced delay-line filter was proposed. A sampled FBG was also used as a multitap photonic transversal filter to implement a classical HT [8]. In [9], a uniform weak-coupling FBG with a  $\pi$ -phase shift in the FBG was proposed to implement a classical HT. Recently, the inverse scattering method has been used to design and fabricate an FBG for classical Hilbert transform [10]. In [11], a wideband HT using a uniform long-period grating (LPG) was proposed. The LPG was designed to have an amplitude-only grating apodization profile with a  $\pi$ -phase shift incorporated in the middle of the grating length. Thanks to the ultra-wide bandwidth of the LPG, a HT with a bandwidth up to terahertz was demonstrated. The major limitation of an FBG- or LPG-based HT or FHT is the lack of tunability. In [12], a Bragg grating written on a planar silicon-on-silicon waveguide was employed to implement a tunable HT. The tuning was realized by incorporating a micro heater in the silicon-on-silica substrate to thermally tune the HT. Instead of using a Bragg grating, in [13] a tunable FHT based on an integrated ring resonator was proposed [13]. Compared with a Bragg grating, a ring resonator with a much smaller footprint occupies much less space on a silicon chip, thus enables integration with a much higher density. Again, the tuning was achieved using a micro heater to tune the coupling coefficient of the ring and correspondingly the phase shift at the resonance wavelength. The major limitation of a tunable HT based on thermal tuning is the relatively slow tuning speed. For thermal tuning, the response time is usually from 1 to 50 ms.

In this letter, we propose a novel method to implement a continuously tunable FHT with a fast tuning speed realized by using a tunable polarizer. The polarization tuning as fast as a few  $\mu\text{s}$  can be achieved. A FHT has an output that is a weighted sum of the original signal and its classical Hilbert-transformed signal. The classical HT is implemented using a  $\pi$ -phase shifted fiber Bragg grating ( $\pi$ -PSFBG). The polarization directions of the original signal and the Hilbert-transformed signal are controlled to be orthogonally polarized. By applying the two signals to a polarizer

Manuscript received June 27, 2013; revised September 16, 2013; accepted October 1, 2013. Date of publication October 4, 2013; date of current version October 23, 2013. This work was supported by the Natural Science and Engineering Research Council of Canada.

The authors are with the Microwave Photonics Research Laboratory, School of Electrical Engineering and Computer Science, University of Ottawa, Ottawa, ON K1N 6N5, Canada (e-mail: jpyao@eecs.uottawa.ca).

Color versions of one or more of the figures in this letter are available online at <http://ieeexplore.ieee.org>.

Digital Object Identifier 10.1109/LPT.2013.2284574

via a polarization controller (PC), the two signals are combined with the weighting coefficients determined by the angle between the principle axis of the polarizer and the polarization direction of the original input signal. A  $\pi$ -PSFBG is fabricated. The performance of the  $\pi$ -PSFBG as a classical HT and the use of the  $\pi$ -PSFBG to implement the proposed FHT is theoretically studied and experimentally evaluated. A continuously tunable FHT with a tunable fractional order of  $\rho = 0.7, 0.86, 0.92, 1, 1.06, 1.17,$  and  $1.24$  to perform Hilbert transformation of a Gaussian pulse with a temporal width of 80 ps is experimentally demonstrated.

## II. PRINCIPLE

The frequency response of a classical HT is expressed as

$$H_C(\omega) = -j\text{sgn}(\omega), \quad (1)$$

where  $\omega$  is the optical frequency, and  $\text{sgn}(\omega)$  is the sign function defined as

$$\text{sgn}(\omega) = \begin{cases} +1, & \omega > 0 \\ 0, & \omega = 0 \\ -1, & \omega < 0. \end{cases} \quad (2)$$

The frequency response of a FHT is given by [2], [14],

$$\begin{aligned} H_F(\omega) &= \begin{cases} e^{-j\varphi}, & \omega > 0 \\ \cos(\varphi), & \omega = 0 \\ e^{+j\varphi}, & \omega < 0 \end{cases} \quad (3) \\ &= \cos(\varphi) + \sin(\varphi)[-j\text{sgn}(\omega)] \\ &= \cos(\varphi) + \sin(\varphi)H_C(\omega), \end{aligned}$$

where  $\varphi = \rho \times \pi/2$  is the phase shift and  $\rho$  is the fractional order. As can be seen a FHT of an order of  $\rho$  has a phase shift of  $(\rho\pi)$  at  $\omega = 0$  with a unity magnitude response. By using (3), the FHT of a signal  $x(t)$  can be expressed as

$$\hat{x}_F(t) = \cos(\varphi)x(t) + \sin(\varphi)\hat{x}_C(t), \quad (4)$$

where  $x(t)$  is the original signal,  $\hat{x}_C(t)$  is the classical Hilbert-transformed signal, and  $\hat{x}_F(t)$  is the fractional-Hilbert-transformed signal with a fractional order of  $\rho$ . From (4) we can see, the fractional Hilbert transformation of a signal has an output that is a weighted sum of the original signal and its classical Hilbert-transformed signal.

For a classical HT, a phase shift of  $\pi$  at  $\omega = 0$  is needed which can be achieved by using a  $\pi$ -PSFBG. A  $\pi$ -PSFBG has a  $\pi$  phase jump at the center wavelength of the notch and a flat magnitude response except the notch, which is ultra narrow and negligible. Thus, the use of a  $\pi$ -PSFBG could perfectly perform a classical HT.

The fractional Hilbert-transformed signal is a weighted sum of the original signal and its classical Hilbert-transformed signal, which can be implemented by making the original signal and its classical Hilbert-transformed signal orthogonally polarized and then combining them at a polarizer. The operation corresponds to achieving a weighted sum of the two signals. By simply tuning the PC before the polarizer, the weighting coefficients are tuned and consequently a FHT with a tunable order is achieved. The principle of our proposed FHT is shown in Fig. 1. As can be seen the original signal and the classical Hilbert-transformed signal are orthogonally

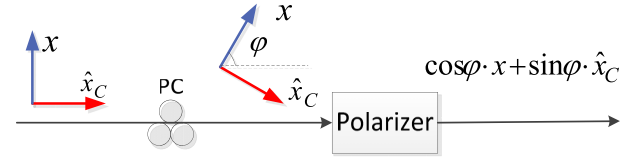


Fig. 1. The proposed tunable fractional Hilbert transformer.

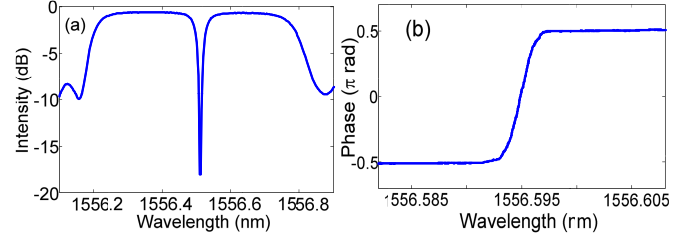


Fig. 2. (a) The reflection spectrum of the fabricated  $\pi$ -PSFBG measured by a LUNA OVA, and (b) the phase response at the notch measured based on the SSB modulation technique [15].

polarized. By tuning the PC, the polarization direction of the original signal will have an angle of  $\varphi$  relative to the principle axis of the polarizer, thus the original signal  $x(t)$  and its classical Hilbert-transformed signal  $\hat{x}_C(t)$  are combined at the output of the polarizer with the weighting coefficients being  $\cos \varphi$  and  $\sin \varphi$ . Since  $\varphi$  is tunable, the two coefficients  $\cos \varphi$  and  $\sin \varphi$  are also tunable. Consequently, a continuously tunable FHT can be achieved.

The classical HT is implemented using a  $\pi$ -PSFBG, which is fabricated in a 5-mm long photosensitive fiber based on the UV scanning beam technique. The uniform phase mask used in the fabrication has a period of 1072 nm. The phase shift at the center of the grating is introduced by moving the phase mask by half of the period, which is mounted on a piezo controller (E-665.CR LVPZT-amplifier/servo). The reflection spectrum of the fabricated  $\pi$ -PSFBG measured by an optical vector analyzer (OVA, LUNA) is shown in Fig. 2(a). Due to the limited resolution of the OVA, the phase response of the  $\pi$ -PSFBG at the notch is measured using a technique based on single sideband (SSB) modulation [15], in which the sideband is moving which is measured by an electrical vector network analyzer (VNA, Agilent E8364A). The measured phase response is shown in Fig. 2(b). As can be seen a phase shift of  $\pi$  is introduced at the notch of the  $\pi$ -PSFBG. Since the magnitude response of the  $\pi$ -PSFBG is flat over a large bandwidth (1556.2 to 1556.8 nm or 75 GHz) with an ultra-narrow notch at the center, the  $\pi$ -PSFBG is suitable for the implementation of a classical HT.

To explore the performance of the fabricated  $\pi$ -PSFBG as a classical HT, a simulation is first performed in which the spectral response of the fabricated  $\pi$ -PSFBG is used and a Gaussian pulse with a temporal width of 100 ps centered at the notch wavelength is used as an input. The signal at the output of the  $\pi$ -PSFBG is simulated which is shown in Fig. 3 (solid line). The signal at the output of an ideal Hilbert transformer is also shown for comparison (dashed line). As can be see the signal from the  $\pi$ -PSFBG is close to that from

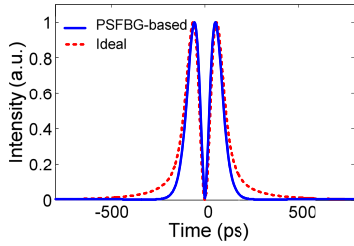


Fig. 3. Simulation results. The signal at the output of the fabricated  $\pi$ -PSFBG when the input is a Gaussian pulse with the temporal width of 100 ps (solid line). The signal at the output of an ideal classical HT is also shown (dashed line).

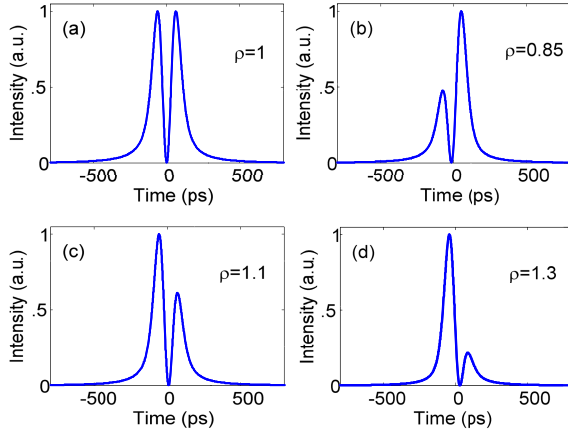


Fig. 4. Simulation results for the proposed FHT for (a)  $\varphi = 90^\circ$ , (b)  $\varphi = 75^\circ$ , (c)  $\varphi = 100^\circ$ , and (d)  $\varphi = 120^\circ$ .

an ideal Hilbert transformer. The small difference is caused by the finite notch of the  $\pi$ -PSFBG. As shown in Fig. 2(a), the magnitude response has a notch which is small, but always exists. The FWHM of the notch is measured to be 5 pm or equivalently 0.6 GHz. The existence of this notch will suppress part of the optical carrier. To minimize the suppression, the  $\pi$ -PSFBG should be improved to have an ultra narrow notch. For example, a  $\pi$ -PSFBG was demonstrated to have a notch of only 2.5 MHz [16]. In addition, the signal carried by the optical carrier may also be partially suppressed, which will cause errors in the Hilbert transformed signal. To evaluate quantitatively the errors, we calculate the root-mean square error (RMSE) between the ideally and the  $\pi$ -PSFBG-based Hilbert transformed signals. The RMSE is about 6%, which is very small.

Then, the use of the  $\pi$ -PSFBG to implement a tunable FHT is simulated. In the simulation, the original signal with a weight of  $\cos(\varphi)$  and the classical Hilbert-transformed signal with a weight of  $\sin(\varphi)$  are added, with the overall output given by  $\hat{x}_\rho(t) = \cos(\varphi)x(t) + \sin(\varphi)\hat{x}_C(t)$ . The simulation results for  $\varphi = 90^\circ, 75^\circ$ , and  $100^\circ$  are shown in Fig. 4. As can be seen the classical HT is achieved when  $\varphi = 90^\circ$ , shown in Fig. 4(a). In this case, only  $\hat{x}_C(t)$  is passing through the polarizer and the order of the FHT is  $\rho = 1$ . When  $\varphi$  is changed, the weight of the classical HT  $\hat{x}_C(t)$  and the original signal  $x(t)$  at the output of the polarizer would be different, thus a FHT with a tunable order is achieved. As can be seen

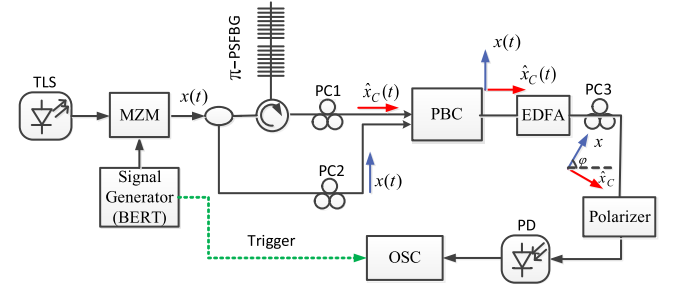


Fig. 5. Experimental setup. TLS: tunable laser source, MZM: Mach-Zehnder modulator, PBC: polarization beam combiner, EDFA: erbium-doped fiber amplifier, PC: polarization controller, PD: photodetector, OSC: oscilloscope.

in Fig. 4(b)–(d), the order of the FHT achieved for  $\varphi = 75^\circ, 100^\circ$  and  $120^\circ$  are  $\rho = 0.85, 1.1$ , and  $1.3$ , respectively. Thus, by continuously tuning  $\varphi$ , a continuously tunable FHT is achieved.

### III. EXPERIMENT

An experiment is performed to validate the proposed FHT. The experimental setup is shown in Fig. 5. A continuous-wave (CW) light generated by a tunable laser source (Anritsu MG9638A) is sent to a Mach-Zehnder modulator (MZM) to which a Gaussian pulse with a temporal width of 80 ps generated by a signal generator (Agilent N4901B) is applied. The optical wavelength is set at 1556.51 nm which is centered at the notch wavelength of the fabricated  $\pi$ -PSFBG. The signal at the output of the MZM is divided into two paths. In the upper path, the optical signal is sent to the fabricated  $\pi$ -PSFBG through a circulator and the reflected signal is sent to a polarization beam combiner (PBC) with the polarization aligned with the slow axis via PC1 to get  $\hat{x}_C(t)$ . In the lower path, the signal at the output of the MZM is sent to the PBC with the polarization aligned with the fast axis path via PC2 to get  $x(t)$ . The lengths of the two paths are controlled very short and balanced, to minimize the optical interference. The powers of  $x(t)$  and  $\hat{x}_C(t)$  are tuned by tuning PC2 and PC1, respectively. The signals along both slow and fast axes are amplified by an erbium-doped fiber amplifier (EDFA) and sent to a polarizer through a third PC (PC3).

As discussed in Section II, by tuning the PC before the polarizer (PC3 in the experimental setup) the weighting coefficients are tunable and thus the order of the FHT is tuned. The signal at the output of the polarizer is detected by a 53-GHz photodetector (PD) and the waveform is observed by a sampling oscilloscope (Agilent 86116A). Fig. 6 shows the experimental results for seven different  $\varphi$  at  $90^\circ, 82^\circ, 96^\circ, 75^\circ, 106^\circ, 62^\circ$ , and  $114^\circ$ . Fig. 6(a) shows the input signal (solid line) from the signal generator which is a bit error tester (BERT) in the experiment. An ideal Gaussian signal is also shown (dashed line). The signal at the output of the FHT with a fractional order of  $\rho = 1, \rho = 0.92, \rho = 1.06, \rho = 0.86, \rho = 1.17, \rho = 0.7$ , and  $\rho = 1.24$  are shown in Fig. 6(b)–(h), respectively. The simulated waveforms for an ideal FHT with an ideal Gaussian input pulse in Fig. 6(a) (dashed line) for the same orders are also shown in

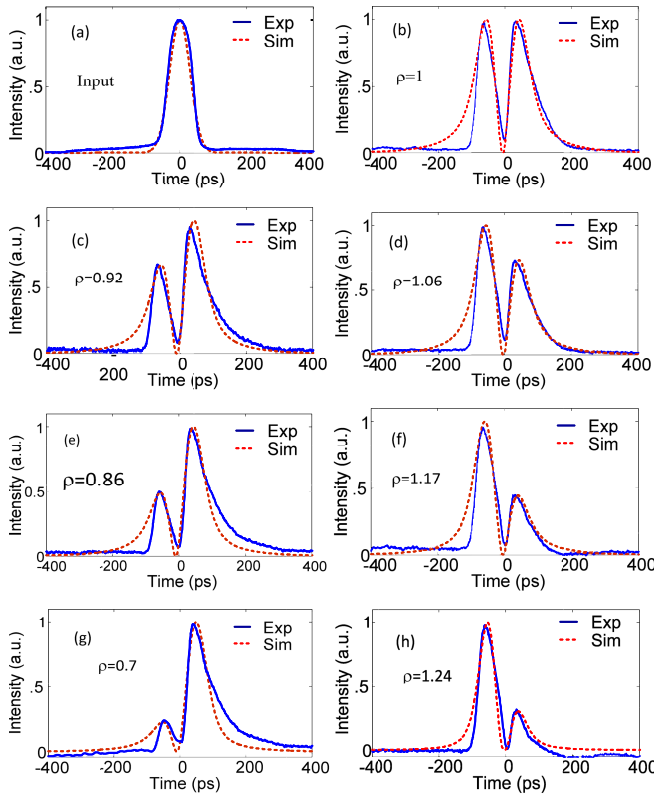


Fig. 6. Simulation and experimental results. (a) An input Gaussian pulse with a FWHM of 80 ps, and the Hilbert-transformed pulses at different orders of (b)  $\rho = 1$ , (c)  $\rho = 0.92$ , (c)  $\rho = 1.06$ , (e)  $\rho = 0.86$ , (f)  $\rho = 1.17$ , (g)  $\rho = 0.7$ , and (h)  $\rho = 1.24$ .

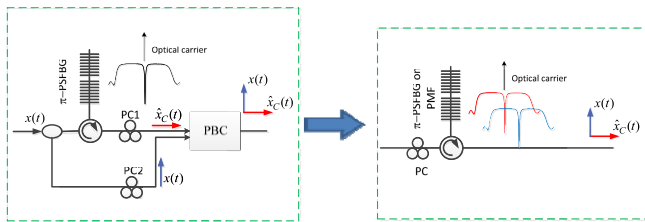


Fig. 7. A simplified implementation, in which the two optical paths are replaced by a single path using a polarization maintaining  $\pi$ -PSFBG.

Fig. 6(b)–(h) as dashed lines. As can be seen a good agreement is achieved. Some small difference between the experimental and simulated results is mainly caused due to the limited bandwidth of the PD (53 GHz).

#### IV. CONCLUSION AND DISCUSSION

Note that the demonstrated system requires physical separation of the two polarizations, which may make the system more complicated with poor stability. In fact, the system can be simplified by using a single path in which the  $\pi$ -PSFBG is written in a polarization maintaining fiber (PMF). The structure is shown in Fig. 7. By using this structure, the interference (which is the main concern of the system stability) is no longer a problem since the two orthogonally polarized signals are traveling in a single path.

In conclusion, a continuously tunable FHT was proposed and experimentally demonstrated using a  $\pi$ -PSFBG. The key contributions of the work was the use of the  $\pi$ -PSFBG to perform a classical HT and the FHT was implemented by combining the original signal and the classical Hilbert-transformed signal through polarization combination, with different combination coefficients corresponding to different fractional orders. A continuously tunable FHT with a tunable fractional order of  $\rho = 0.7, 0.86, 0.92, 1, 1.06, 1.17$ , and  $1.24$  to perform Hilbert transformation of a Gaussian pulse with a temporal width of 80 ps was experimentally demonstrated.

#### REFERENCES

- [1] S. L. Hahn and A. D. Poularikas, *Transforms and Applications Handbook*, 3rd ed. Boca Raton, FL, USA: CRC Press, 2010, Ch. 7.
- [2] A. W. Lohmann, D. Mendlovic, and Z. Zalevsky, "Fractional Hilbert transform," *Opt. Lett.*, vol. 21, no. 4, pp. 281–283, Feb. 1996.
- [3] C. S. Guo, Y. J. Han, J. B. Xu, and J. Ding, "Radial Hilbert transform with Laguerre-Gaussian spatial filters," *Opt. Lett.*, vol. 31, no. 10, pp. 1394–1396, May 2006.
- [4] H. Emami, N. Sarkhosh, L. A. Bui, and A. Mitchell, "Wideband RF photonic in-phase and quadrature-phase generation," *Opt. Lett.*, vol. 33, no. 2, pp. 98–100, Jan. 2008.
- [5] H. Emami, N. Sarkhosh, L. A. Bui, and A. Mitchell, "Amplitude independent RF instantaneous frequency measurement system using photonic Hilbert transform," *Opt. Express*, vol. 16, no. 18, pp. 13707–13712, Sep. 2008.
- [6] Z. Li, W. Li, H. Chi, X. Zhang, and J. P. Yao, "A continuously tunable microwave fractional Hilbert transformer based on a photonic microwave delay-line filter using a polarization modulator," *IEEE Photon. Technol. Lett.*, vol. 23, no. 22, pp. 1694–1699, Nov. 15, 2011.
- [7] Z. Li, Y. Han, H. Chi, X. Zhang, and J. P. Yao, "A continuously tunable microwave fractional Hilbert transformer based on a nonuniformly spaced photonic microwave delay-line filter," *J. Lightw. Technol.*, vol. 30, no. 12, pp. 1948–1953, Jun. 15, 2012.
- [8] X. Y. Wang, M. Hanawa, K. Nakamura, K. Talkano, and K. Nakagawa, "Sideband suppression characteristics of optical SSB generation filter with sampled FBG based 4-taps optical Hilbert transformer," in *Proc. APCC*, 2009, pp. 622–625.
- [9] M. H. Asghari and J. Azaña, "All-optical Hilbert transformer based on a single phase-shifted fiber Bragg grating: Design and analysis," *Opt. Lett.*, vol. 34, no. 3, pp. 334–336, Feb. 2009.
- [10] M. Li and J. P. Yao, "Experimental demonstration of a wideband photonic temporal Hilbert transformer based on a single fiber Bragg grating," *IEEE Photon. Technol. Lett.*, vol. 22, no. 21, pp. 1559–1561, Nov. 1, 2010.
- [11] R. Ashrafi and J. Azaña, "Terahertz bandwidth all-optical Hilbert transformers based on long-period gratings," *Opt. Lett.*, vol. 37, no. 13, pp. 2604–2606, Jul. 2012.
- [12] C. Sima, J. C. Gates, H. L. Rogers, P. L. Mennea, C. Holmes, M. N. Zervas, and P. G. R. Smith, "Phase controlled integrated interferometric single-sideband filter based on planar Bragg gratings implementing photonic Hilbert transform," *Opt. Lett.*, vol. 38, no. 5, pp. 727–729, Mar. 2013.
- [13] L. Zhuang, M. R. Khan, W. Becker, A. Leinse, R. Heideman, and C. Roeloffzen, "Novel microwave photonic fractional Hilbert transformer using a ring resonator-based optical all-pass filter," *Opt. Express*, vol. 20, no. 24, pp. 26499–26510, Nov. 2012.
- [14] W. K. Frederick, *Hilbert Transforms*, vol. 1, Cambridge, U.K.: Cambridge Univ. Press, 2009, Ch. 1.
- [15] Z. Tang, S. Pan, and J. P. Yao, "A high resolution optical vector network analyzer based on a wideband and wavelength-tunable optical single-sideband modulator," *Opt. Express*, vol. 20, no. 6, pp. 6555–6560, Mar. 2012.
- [16] X. Chen, J. P. Yao, F. Zeng, and Z. Deng, "Single-longitudinal-mode fiber ring laser employing an equivalent phase-shift fiber Bragg grating," *IEEE Photon. Technol. Lett.*, vol. 17, no. 7, pp. 1390–1392, Jul. 2005.